

# SUPPORTING INFORMATION

FOR

# Pseudo-octahedral Nickel(II) Complexes of Strongly Absorbing Benzannulated Pincer-Type Amido Ligands: Ligand-Based Redox and non- Aufbau Electronic Behaviour

Jason D. Braun,<sup>a</sup> Issiah B. Lozada,<sup>a</sup> Michael Shepit,<sup>b</sup> Johan van Lierop<sup>b</sup> and David E. Herbert <sup>a\*</sup>

<sup>a</sup> Department of Chemistry and the Manitoba Institute of Materials, University of Manitoba, 144 Dysart Road, Winnipeg, MB, R3T 2N2, Canada

<sup>b</sup> Department of Physics and Astronomy, University of Manitoba, 31A Sifton Rd, Winnipeg,  
MB, Canada, R3T 2N2

\*david.herbert@umanitoba.ca

## Table of Contents

<b>Figure S1.</b> $^1\text{H}$ NMR (300 MHz, $\text{CDCl}_3$ , 25°C) of $(^{\text{CF}_3}\text{L})_2\text{Ni}$ .	4
<b>Figure S2.</b> $^1\text{H}$ NMR (300 MHz, $\text{CDCl}_3$ , 25°C) of $(^{\text{C}_1}\text{L})_2\text{Ni}$ .	4
<b>Figure S3.</b> Evans' method NMR (300 MHz, $\text{CDCl}_3$ , 25°C) of $(^{\text{CF}_3}\text{L})_2\text{Ni}$ .	5
<b>Figure S4.</b> Evans' method NMR (300 MHz, $\text{CDCl}_3$ , 25°C) of $(^{\text{C}_1}\text{L})_2\text{Ni}$ .	5
<b>Figure S5.</b> $1/\chi$ plot for $(^{\text{tBu}}\text{L})_2\text{Ni}$ .	6
<b>Figure S6.</b> $1/\chi$ plot for $(^{\text{CF}_3}\text{L})_2\text{Ni}$ .	7
<b>Figure S7.</b> $1/\chi$ plot for $(^{\text{C}_1}\text{L})_2\text{Ni}$ .	8
<b>Table S1.</b> Selected bond distances ( $\text{\AA}$ ) and angles ( $^\circ$ ) for $(^{\text{R}}\text{L})_2\text{Ni}$ complexes.	9
<b>Table S2.</b> Crystal structure and optimized (SMD-O3LYP/6-31+G(d,p)) ground state geometric parameters for $(^{\text{R}}\text{L})_2\text{Ni}$ .	10
<b>Table S3.</b> Fragment contributions (%) to selected ground state ROKS MOs of $(^{\text{CF}_3}\text{L})_2\text{Ni}$ (Figure 6) using Hirshfeld atomic population method (SMD-roPBE0/6-31+G(d,p)//SMD-uO3LYP/6-31+G(d,p)).	10
<b>Figure S8.</b> Ground state spin density isosurfaces (isovalue = 0.004) and Mulliken spin density on Ni for $(^{\text{CF}_3}\text{L})_2\text{Ni}$ and $(^{\text{C}_1}\text{L})_2\text{Ni}$ (SMD-uPBE0/6-31+G(d,p)//SMD-uO3LYP/6-31+G(d,p)).	11
<b>Figure S9.</b> Selected molecular orbital isosurfaces (isovalue = 0.04; SMD-uPBE0/6-31+G(d,p)//SMD-uO3LYP/6-31+G(d,p)) and electron-hole density maps (isovalue = 0.002; green = electron, blue = hole) for the lowest energy transitions in $(^{\text{CF}_3}\text{L})_2\text{Ni}$ ( $E < 3 \text{ eV}$ ).	11
<b>Table S4.</b> Fragment contributions ( $\alpha/\theta$ ; %) to selected ground state UKS MOs of $(^{\text{CF}_3}\text{L})_2\text{Ni}$ using Hirshfeld atomic population method (SMD-uPBE0/6-31+G(d,p)//SMD-uO3LYP/6-31+G(d,p)).	12
<b>Figure S10.</b> Selected molecular orbital isosurfaces (isovalue = 0.04; SMD-uPBE0/6-31+G(d,p)//SMD-uO3LYP/6-31+G(d,p)) and electron-hole density maps (isovalue = 0.002; green = electron, blue = hole) for the lowest energy transitions in $(^{\text{C}_1}\text{L})_2\text{Ni}$ ( $E < 3 \text{ eV}$ ).	12
<b>Table S5.</b> Fragment contributions ( $\alpha/\theta$ ; %) to selected ground state UKS MOs of $(^{\text{C}_1}\text{L})_2\text{Ni}$ using Hirshfeld atomic population method (SMD-uPBE0/6-31+G(d,p)//SMD-uO3LYP/6-31+G(d,p)).	13
<b>Figure S11.</b> TD-DFT simulated spectrum (---) and vertical excitation energies (red) superimposed on the experimental spectrum (-) of $(^{\text{CF}_3}\text{L})_2\text{Ni}$ in $\text{CH}_3\text{CN}$ (TD-SMD-uPBE0/6-31+G(d,p)//SMD-uO3LYP/6-31+G(d,p)); FWHM = $3000 \text{ cm}^{-1}$ ; $f > 0.05$ ).	13
<b>Table S6.</b> TDDFT predicted vertical excitation energies, oscillator strengths ( $f_{\text{osc}} > 0.05$ ), and MO contributions (> 10%) $(^{\text{CF}_3}\text{L})_2\text{Ni}$ (TD-SMD-uPBE0/6-31+G(d,p)//SMD-uO3LYP/6-31+G(d,p)); FWHM = $3000 \text{ cm}^{-1}$ ; $f > 0.05$ ).	14

<i>Figure S12. TD-DFT simulated spectrum (---) and vertical excitation energies (red) superimposed on the experimental spectrum (-) of (<sup>C</sup>L)<sub>2</sub>Ni in CH<sub>3</sub>CN (TD-SMD-uPBE0/6-31+G(d,p)//SMD-uO3LYP/6-31+G(d,p)); FWHM = 3000 cm<sup>-1</sup>; f &gt; 0.05).</i>	15
<i>Table S7. TDDFT predicted vertical excitation energies, oscillator strengths (f<sub>osc</sub> &gt; 0.05), and MO contributions (&gt; 10%) (<sup>C</sup>L)<sub>2</sub>Ni (TD-SMD-uPBE0/6-31+G(d,p)//SMD-uO3LYP/6-31+G(d,p)).</i>	16
<i>Equations – IVCT Marcus-Hush Analysis</i>	16
<i>Figure S13. <sup>1</sup>H NMR (300 MHz, CDCl<sub>3</sub>, 25°C) of 4-nitro-2-chlorophenanthridine (1c).</i>	17
<i>Figure S14. <sup>13</sup>C{<sup>1</sup>H} NMR (75 MHz, CDCl<sub>3</sub>, 25°C) of 4-nitro-2-chlorophenanthridine (1c).</i>	17
<i>Figure S15. <sup>1</sup>H NMR (300 MHz, CDCl<sub>3</sub>, 25°C) of 4-amino-2-chlorophenanthridine (1e).</i>	18
<i>Figure S16. <sup>13</sup>C{<sup>1</sup>H} NMR (75 MHz, CDCl<sub>3</sub>, 25°C) of 4-amino-2-chlorophenanthridine (1e).</i>	18
<i>Figure S17. <sup>1</sup>H NMR (500 MHz, CDCl<sub>3</sub>, 25°C) of <sup>Cl-Phen</sup>NN(H)N<sup>Quin</sup> (L3).</i>	19
<i>Figure S18. <sup>13</sup>C{<sup>1</sup>H} NMR (125 MHz, CDCl<sub>3</sub>, 25°C) of <sup>Cl-Phen</sup>NN(H)N<sup>Quin</sup> (L3).</i>	19
<i>Figure S19. <sup>1</sup>H-<sup>1</sup>H COSY NMR (500/125 MHz, CDCl<sub>3</sub>, 25°C) of <sup>Cl-Phen</sup>NN(H)N<sup>Quin</sup> (L3).</i>	20
<i>Figure S20. HSQC NMR (500/125 MHz, CDCl<sub>3</sub>, 25°C) of <sup>Cl-Phen</sup>NN(H)N<sup>Quin</sup> (L3).</i>	20
<i>Figure S21. HMBC NMR (500/125 MHz, CDCl<sub>3</sub>, 25°C) of <sup>Cl-Phen</sup>NN(H)N<sup>Quin</sup> (L3).</i>	21
<i>Figure S22. HR-MS of (<sup>CF<sub>3</sub></sup>L)<sub>2</sub>Ni.</i>	22
<i>Figure S23. HR-MS of (<sup>C</sup>L)<sub>2</sub>Ni.</i>	23
<i>Energies and Reaction Coordinates</i>	24

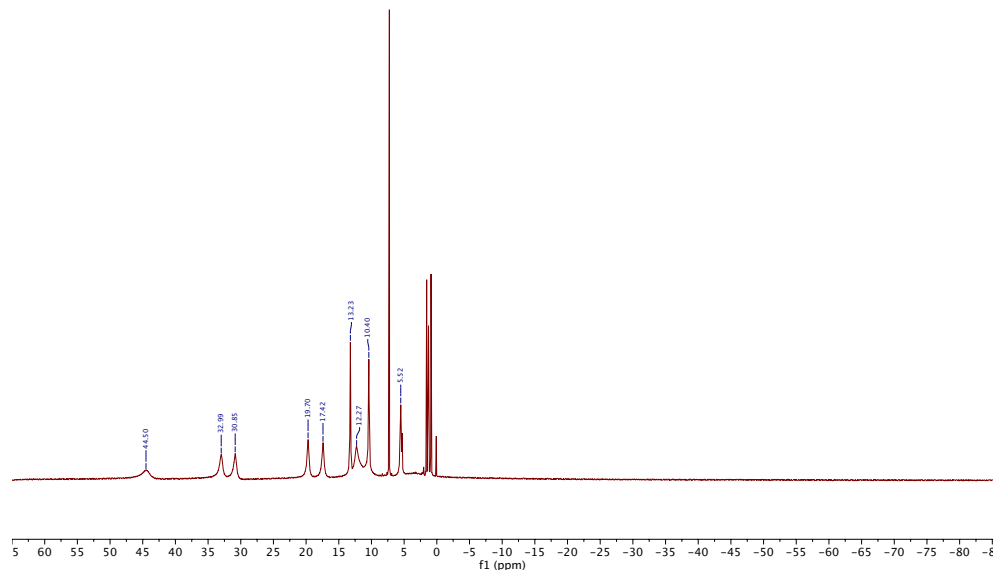


**Figure S1.** <sup>1</sup>H NMR (300 MHz, CDCl<sub>3</sub>, 25°C) of (CF<sub>3</sub>L)<sub>2</sub>Ni.

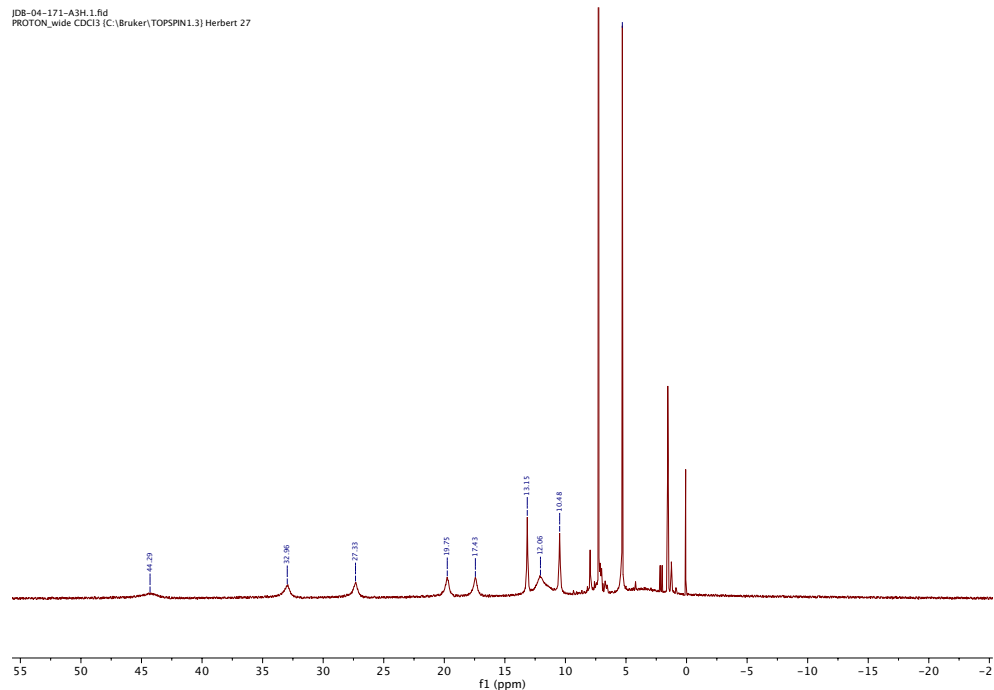


**Figure S2.** <sup>1</sup>H NMR (300 MHz, CDCl<sub>3</sub>, 25°C) of (ClL)<sub>2</sub>Ni.

JDB-04-170-E3H.1.fid  
Evans method  
PROTON CDCl<sub>3</sub> (C:\Bruker\TOPSPIN1.3) Herbert 24

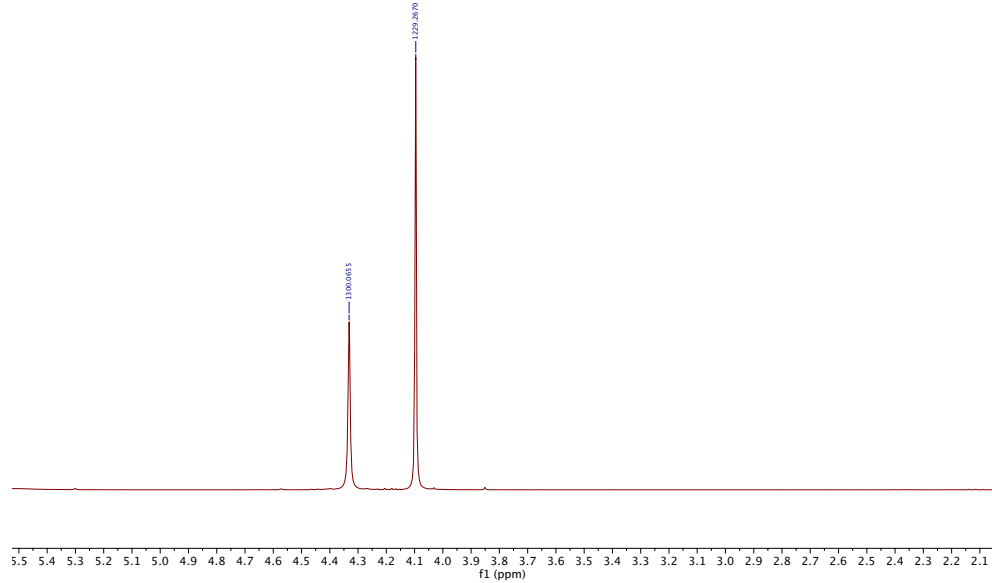


**Figure S3.** Evans' method NMR (300 MHz, CDCl<sub>3</sub>, 25°C) of (CF<sub>3</sub>L)<sub>2</sub>Ni.

JDB-04-171-D3H.1.fid  
Evans method  
PROTON CDCl<sub>3</sub> (C:\Bruker\TOPSPIN1.3) Herbert 49

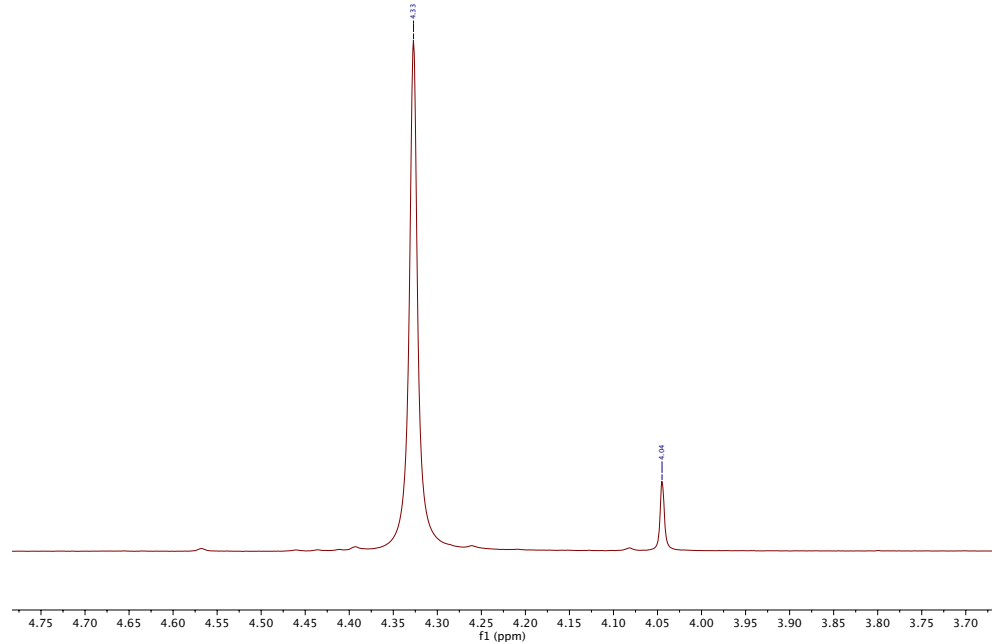


**Figure S4.** Evans' method NMR (300 MHz, CDCl<sub>3</sub>, 25°C) of (ClL)<sub>2</sub>Ni.

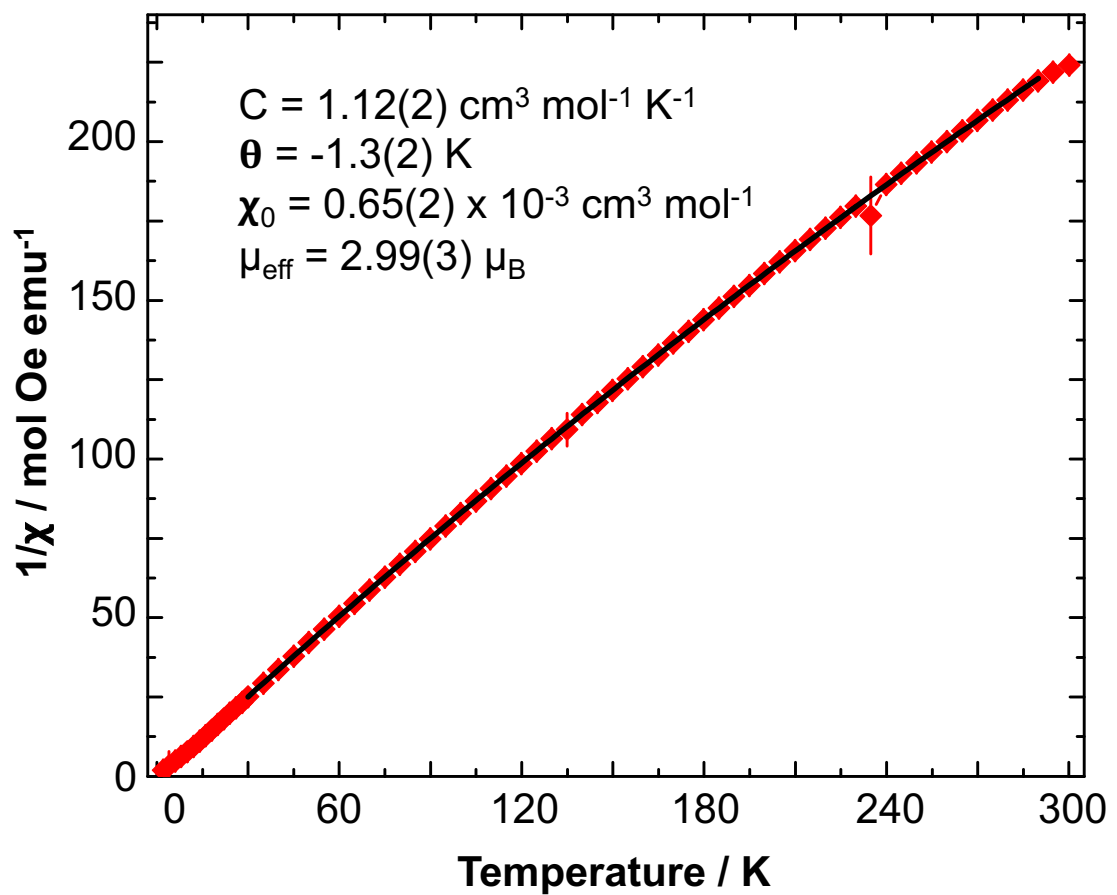


**Figure S5.**  $1/\chi$  plot for  $(t\text{BuL})_2\text{Ni}$ .

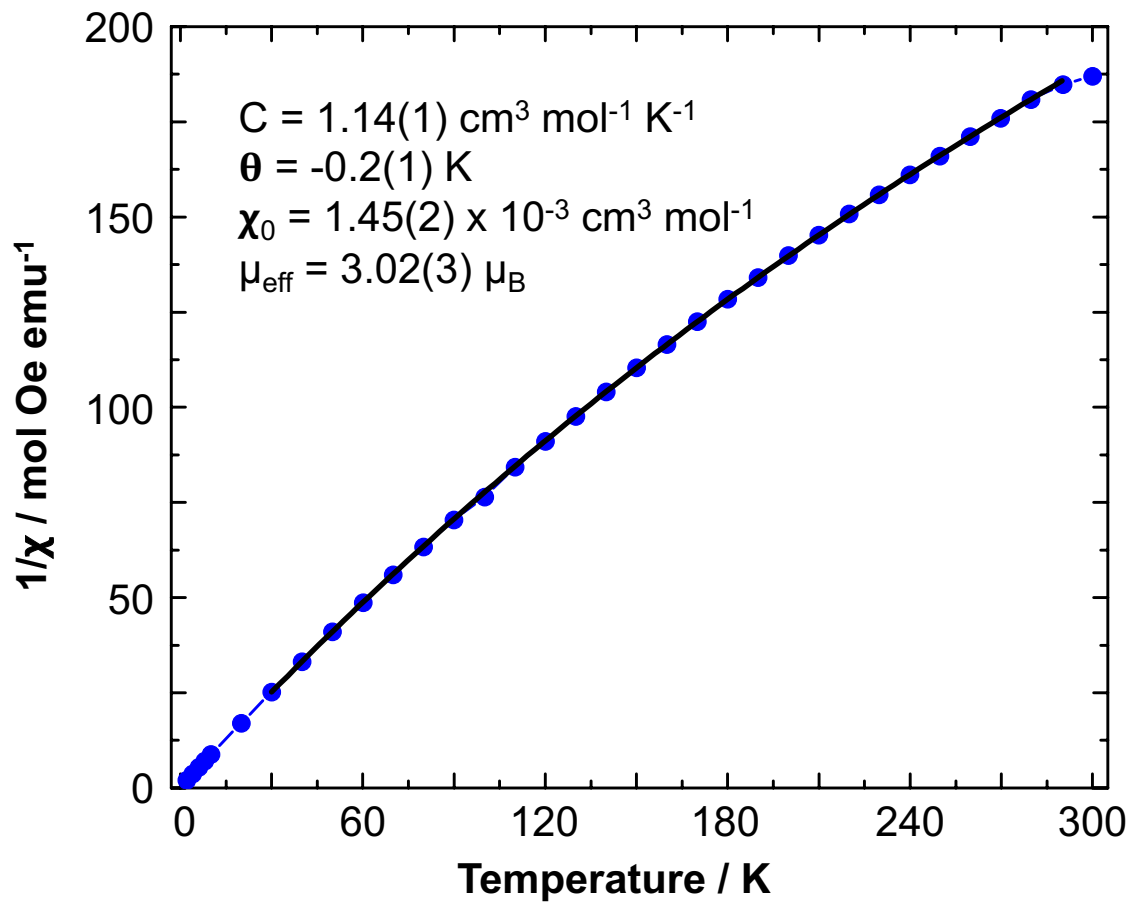


**Figure S6.**  $1/\chi$  plot for  $(\text{CF}_3\text{L})_2\text{Ni}$ .

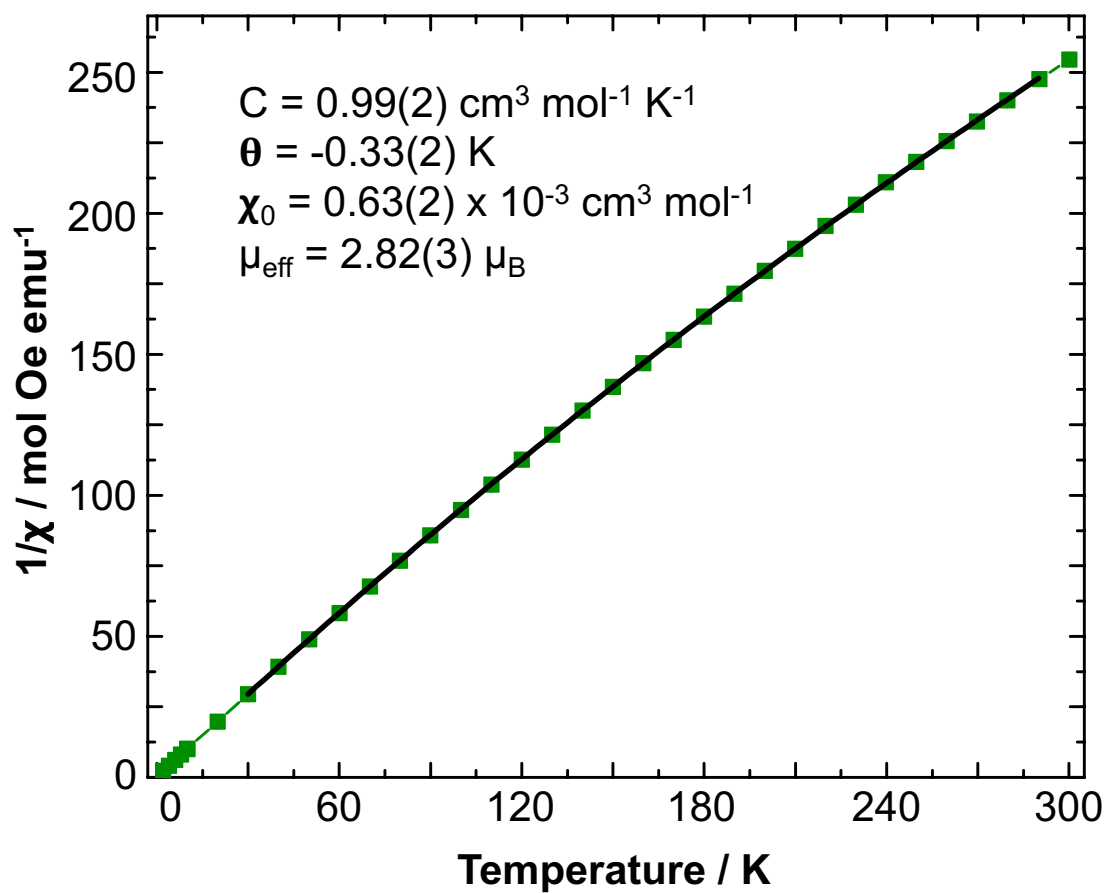


**Figure S7.**  $1/\chi$  plot for  $(\text{ClL})_2\text{Ni}$ .

**Table S1.** Selected bond distances (Å) and angles (°) for (<sup>R</sup>L)<sub>2</sub>Ni complexes.

	( <sup>Bu</sup> L) <sub>2</sub> Ni	( <sup>CF<sub>3</sub></sup> L) <sub>2</sub> Ni	( <sup>Cl</sup> L) <sub>2</sub> Ni
<b><i>Ni – N<sub>phen</sub></i></b>			
Ni – N1	2.0707(13)	2.0830(19)	2.088(3)
Ni – N4	2.0789(13)	2.0728(19)	2.066(3)
<b><i>Ni – N<sub>amido</sub></i></b>			
Ni – N2	2.0168(13)	2.0163(18)	2.000(3)
Ni – N5	2.0161(13)	2.0142(18)	2.014(3)
<b><i>Ni – N<sub>quin</sub></i></b>			
Ni – N3	2.0766(14)	2.0797(19)	2.091(4)
Ni – N6	2.0721(13)	2.0790(19)	2.060(3)
<b><i>N<sub>phen</sub> – C<sup>a</sup></i></b>			
N1 – C1	1.310(2)	1.302(3)	1.289(5)
N4 – C27	1.3047(19)	1.302(3)	1.300(4)
N4 – C24			
N4 – C23			
<b><i>Intraligand angles</i></b>			
N1 – Ni – N3	159.75(5)	159.28(7)	159.41(14)
N1 – Ni – N2	80.09(5)	79.38(7)	79.81(14)
N2 – Ni – N3	79.72(5)	79.91(8)	79.68(17)
N4 – Ni – N6	160.26(5)	159.69(7)	160.52(11)
N4 – Ni – N5	80.00(5)	79.78(7)	80.18(11)
N5 – Ni – N6	80.28(5)	79.98(7)	80.51(11)
<b><i>Interligand angles</i></b>			
N2 – Ni – N5	178.25(5)	177.04(7)	178.83(13)
N1 – Ni – N6	91.84(5)	92.18(7)	91.50(12)
N2 – Ni – N4	98.36(5)	102.75(8)	98.71(12)
N2 – Ni – N6	101.37(5)	97.53(8)	100.61(13)
N1 – Ni – N5	100.51(5)	99.04(7)	100.54(11)
N3 – Ni – N5	99.72(5)	101.67(8)	99.94(14)
N3 – Ni – N4	93.42(5)	91.40(8)	91.81(11)

<sup>a</sup> “Imine-like” (C=N) carbon adjacent to N(1) and N(4) in the phenanthridine arm, labeled C27 in (<sup>Bu</sup>L)<sub>2</sub>Ni, C24 in (<sup>CF<sub>3</sub></sup>L)<sub>2</sub>Ni and C23 in (<sup>Cl</sup>L)<sub>2</sub>Ni

**Table S2.** Crystal structure and optimized (SMD-O3LYP/6-31+G(d,p)) ground state geometric parameters for (<sup>R</sup>L)<sub>2</sub>Ni.

	( <sup>t</sup> BuL) <sub>2</sub> Ni		( <sup>CF</sup> <sub>3</sub> L) <sub>2</sub> Ni		( <sup>Cl</sup> L) <sub>2</sub> Ni	
Bond / Å	XRD	DFT	XRD	DFT	XRD	DFT
Ni-N <sub>amide,1</sub>	<b>2.017</b>	<b>2.043</b>	<b>2.016</b>	<b>2.038</b>	<b>2.000</b>	<b>2.042</b>
Ni-N <sub>amide,2</sub>	<b>2.016</b>	<b>2.043</b>	<b>2.014</b>	<b>2.038</b>	<b>2.014</b>	<b>2.042</b>
Ni-N <sub>phen,1</sub>	<b>2.071</b>	<b>2.130</b>	<b>2.083</b>	<b>2.137</b>	<b>2.088</b>	<b>2.132</b>
Ni-N <sub>phen,2</sub>	<b>2.078</b>	<b>2.131</b>	<b>2.073</b>	<b>2.137</b>	<b>2.066</b>	<b>2.132</b>
Ni-N <sub>quin,1</sub>	<b>2.076</b>	<b>2.135</b>	<b>2.080</b>	<b>2.135</b>	<b>2.091</b>	<b>2.133</b>
Ni-N <sub>quin,2</sub>	<b>2.072</b>	<b>2.134</b>	<b>2.079</b>	<b>2.135</b>	<b>2.060</b>	<b>2.129</b>
Angle / °						
N <sub>amide,1</sub> - Ni-N <sub>amide,2</sub>	<b>178.2</b>	<b>179.8</b>	<b>177.0</b>	<b>179.3</b>	<b>178.8</b>	<b>179.6</b>
N <sub>phen,1</sub> - Ni-N <sub>phen,2</sub>	<b>91.0</b>	<b>91.0</b>	<b>92.7</b>	<b>92.4</b>	<b>89.6</b>	<b>92.0</b>
N <sub>quin,1</sub> - Ni-N <sub>quin,2</sub>	<b>90.6</b>	<b>90.6</b>	<b>91.0</b>	<b>92.6</b>	<b>94.0</b>	<b>92.2</b>
N <sub>phen</sub> - Ni-N <sub>quin</sub>	<b>160.1</b>	<b>160.0</b>	<b>159.5</b>	<b>157.5</b>	<b>160.0</b>	<b>157.9</b>

**Table S3.** Fragment contributions (%) to selected ground state ROKS MOs of (<sup>CF</sup><sub>3</sub>L)<sub>2</sub>Ni (**Figure 6**) using Hirshfeld atomic population method (SMD-roPBE0/6-31+G(d,p)//SMD-uO3LYP/6-31+G(d,p)).

MO	Ni	N <sub>amide</sub>	HC=N <sup>phen</sup>	HC=N <sup>quin</sup>	Ar <sup>phen</sup>	Ar <sup>quin</sup>	CF <sub>3</sub>
LUMO	2	1	26	6	45	17	2
SOMO (d <sub>z<sup>2</sup></sub> )	80	9	3	3	2	2	0
SOMO (d <sub>x<sup>2</sup>-y<sup>2</sup></sub> )	84	0	6	6	1	1	0
HOMO (n <sub>N,am</sub> <sup>π</sup> )	4	20	3	3	32	37	0
H-1 (n <sub>N,am</sub> <sup>π</sup> )	2	21	3	3	32	38	0

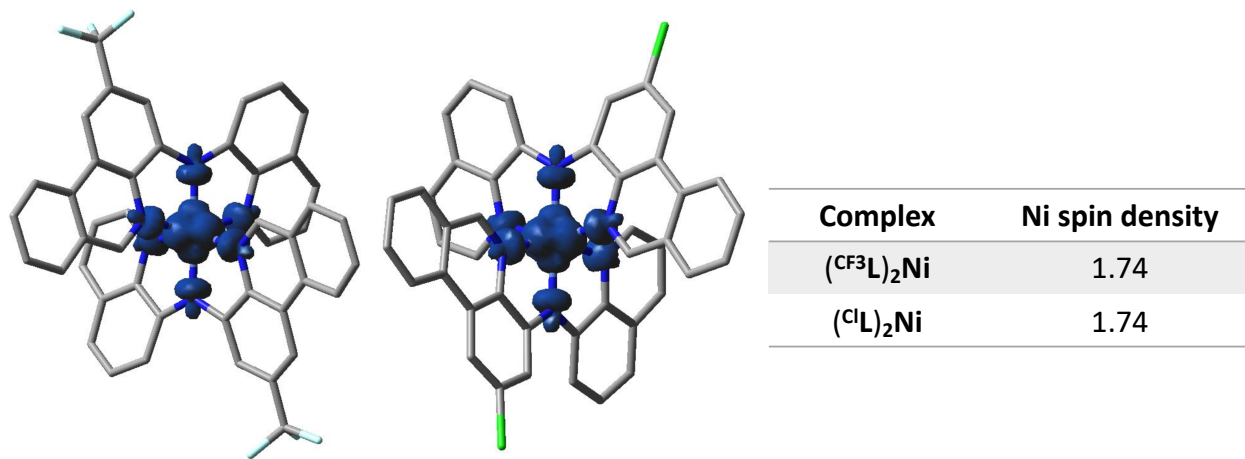


**Figure S8.** Ground state spin density isosurfaces (iso value = 0.004) and Mulliken spin density on Ni for  $(^{CF_3}L)_2Ni$  and  $(^CL)_2Ni$  (SMD-uPBE0/6-31+G(d,p)//SMD-uO3LYP/6-31+G(d,p)).

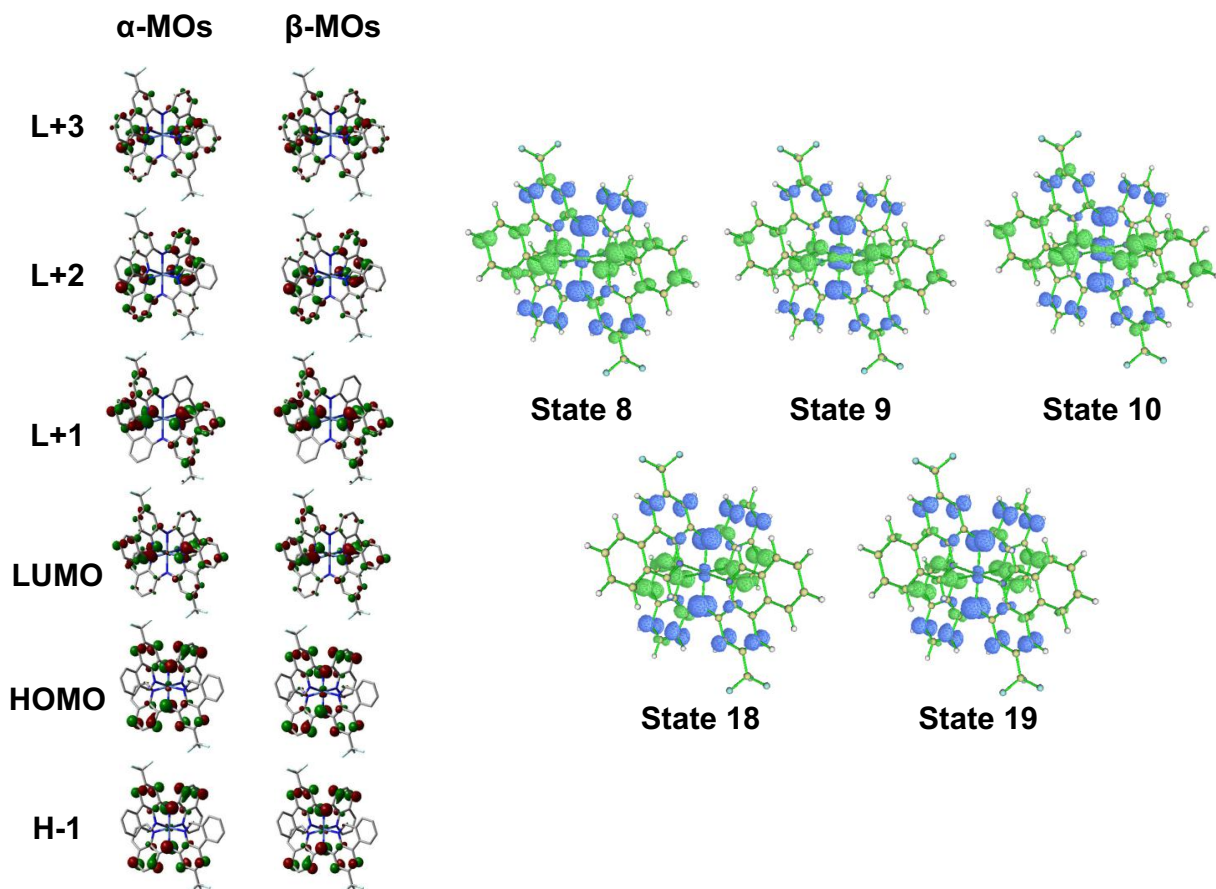


**Figure S9.** Selected molecular orbital isosurfaces (iso value = 0.04; SMD-uPBE0/6-31+G(d,p)//SMD-uO3LYP/6-31+G(d,p)) and electron-hole density maps (iso value = 0.002; green = electron, blue = hole) for the lowest energy transitions in  $(^{CF_3}L)_2Ni$  ( $E < 3$  eV).

**Table S4.** Fragment contributions ( $\alpha/\beta$ ; %) to selected ground state UKS MOs of  $(^{CF_3}L)_2Ni$  using Hirshfeld atomic population method (SMD-uPBE0/6-31+G(d,p)//SMD-uO3LYP/6-31+G(d,p)).

MO	Ni	N <sup>amide</sup>	HC=N <sup>phen</sup>	HC=N <sup>quin</sup>	Ar <sup>phen</sup>	Ar <sup>quin</sup>	CF <sub>3</sub>
<b>L+3</b>	1/1	1/1	8/7	18/17	33/36	38/36	1/1
<b>L+2</b>	1/1	2/2	1/2	23/22	18/21	54/52	0/0
<b>L+1</b>	1/1	1/1	32/31	1/1	58/58	4/5	3/3
<b>LUMO</b>	1/2	1/1	26/25	6/6	46/46	18/18	2/2
<b>HOMO</b>	3/5	20/20	3/3	3/3	32/32	38/37	0/0
<b>H-1</b>	2/3	21/21	3/3	3/3	32/32	38/37	0/0

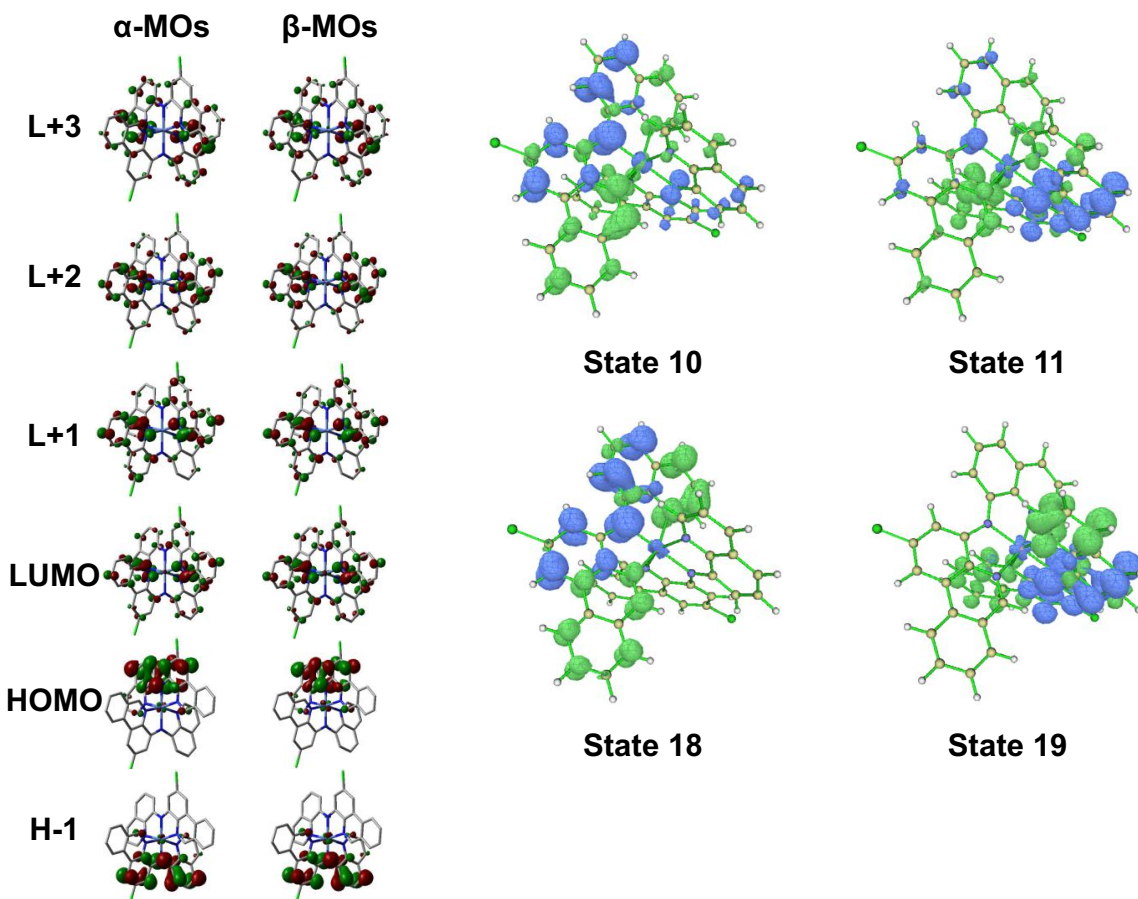


**Figure S10.** Selected molecular orbital isosurfaces (isovalue = 0.04; SMD-uPBE0/6-31+G(d,p)//SMD-uO3LYP/6-31+G(d,p)) and electron-hole density maps (isovalue = 0.002; green = electron, blue = hole) for the lowest energy transitions in  $(^{Cl}L)_2Ni$  ( $E < 3$  eV).

**Table S5.** Fragment contributions ( $\alpha/\beta$ ; %) to selected ground state UKS MOs of  $(^{Cl}L)_2Ni$  using Hirshfeld atomic population method (SMD-uPBE0/6-31+G(d,p)//SMD-uO3LYP/6-31+G(d,p)).

MO	Ni	N <sup>amide</sup>	HC=N <sup>phen</sup>	HC=N <sup>quin</sup>	Ar <sup>phen</sup>	Ar <sup>quin</sup>	Cl
<b>L+3</b>	1/1	1/1	7/7	19/17	29/33	43/39	0/0
<b>L+2</b>	1/1	1/1	13/13	16/15	36/39	32/30	1/1
<b>L+1</b>	1/1	1/1	27/26	4/5	51/49	15/17	1/1
<b>LUMO</b>	1/2	1/1	22/22	9/9	40/40	25/25	1/1
<b>HOMO</b>	2/4	20/20	4/4	3/3	34/33	37/36	0/0
<b>H-1</b>	2/4	20/20	4/4	3/3	34/33	37/36	0/0

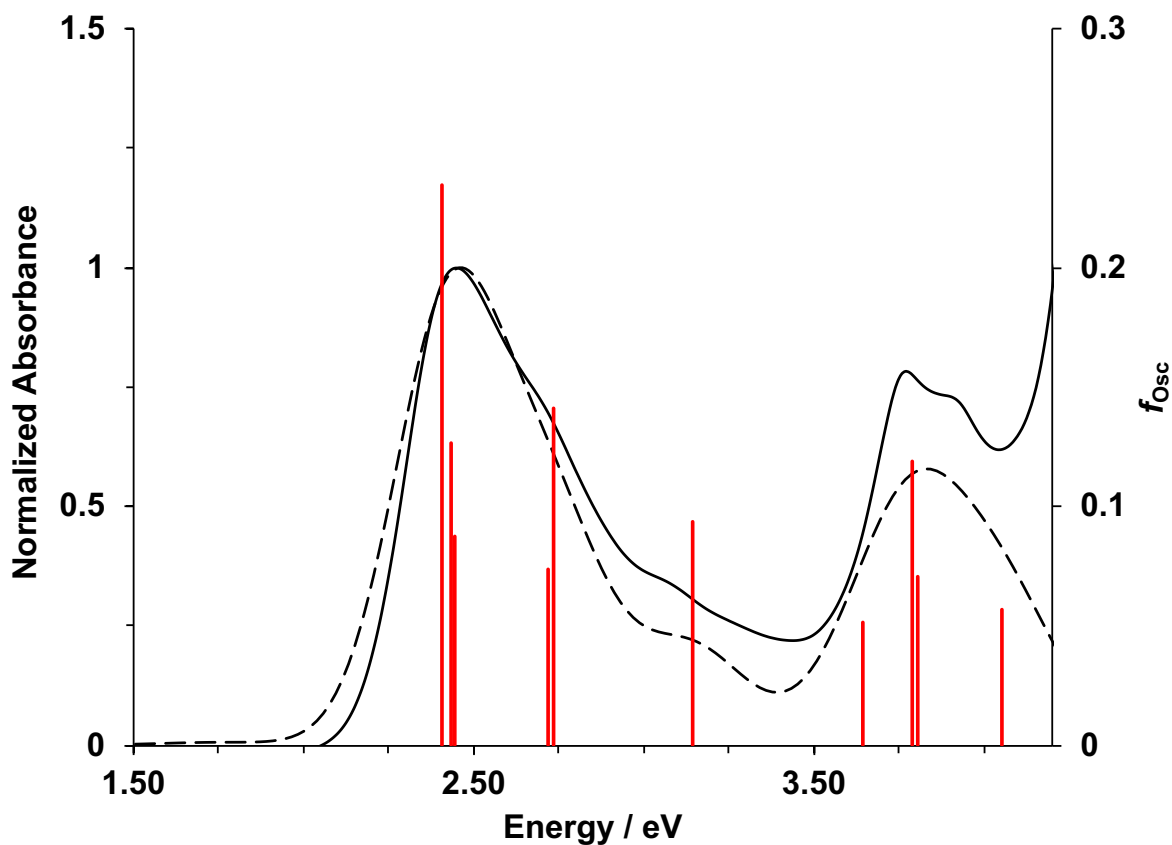


**Figure S11.** TD-DFT simulated spectrum (---) and vertical excitation energies (red) superimposed on the experimental spectrum (-) of  $(^{CF_3}L)_2Ni$  in  $CH_3CN$  (TD-SMD-uPBE0/6-31+G(d,p)//SMD-uO3LYP/6-31+G(d,p)); FWHM =  $3000\text{ cm}^{-1}$ ;  $f > 0.05$ ).

**Table S6.** TDDFT predicted vertical excitation energies, oscillator strengths ( $f_{\text{osc}} > 0.05$ ), and MO contributions (> 10%) ( $\text{CF}_3\text{L}$ )<sub>2</sub>Ni (TD-SMD-uPBE0/6-31+G(d,p)//SMD-uO3LYP/6-31+G(d,p)); FWHM = 3000 cm<sup>-1</sup>;  $f > 0.05$ ).

No.	E / eV	$f_{\text{osc}}$	Major contribs
<b>8</b>	2.40	0.23	HOMO(A)→LUMO(A) (38%), HOMO(B)→LUMO(B) (53%)
<b>9</b>	2.43	0.13	H-1(A)→LUMO(A) (17%), HOMO(A)→L+1(A) (10%), H-1(B)→LUMO(B) (34%)
<b>10</b>	2.44	0.09	H-1(A)→LUMO(A) (11%), HOMO(A)→L+1(A) (14%), HOMO(B)→L+1(B) (44%)
<b>18</b>	2.72	0.07	H-1(A)→L+3(A) (11%), HOMO(A)→L+2(A) (35%), HOMO(B)→L+2(B) (47%)
<b>19</b>	2.74	0.14	H-1(A)→L+2(A) (19%), HOMO(A)→L+3(A) (29%), HOMO(B)→L+3(B) (41%)
<b>30</b>	3.14	0.09	H-1(A)→L+4(A) (17%), HOMO(A)→L+5(A) (33%), H-1(B)→L+4(B) (11%), HOMO(B)→L+5(B) (30%)
<b>46</b>	3.64	0.05	H-1(A)→L+7(A) (22%), HOMO(A)→L+6(A) (20%), H-1(B)→L+7(B) (15%), HOMO(B)→L+6(B) (18%), HOMO(B)→L+8(B) (10%)
<b>51</b>	3.79	0.12	H-1(A)→L+8(A) (12%), HOMO(A)→L+6(A) (14%), HOMO(A)→L+9(A) (15%), HOMO(B)→L+6(B) (30%)
<b>52</b>	3.80	0.07	H-3(A)→L+1(A) (13%), H-1(A)→L+6(A) (13%), HOMO(A)→L+8(A) (17%), H-1(B)→L+6(B) (25%), HOMO(B)→L+9(B) (12%)

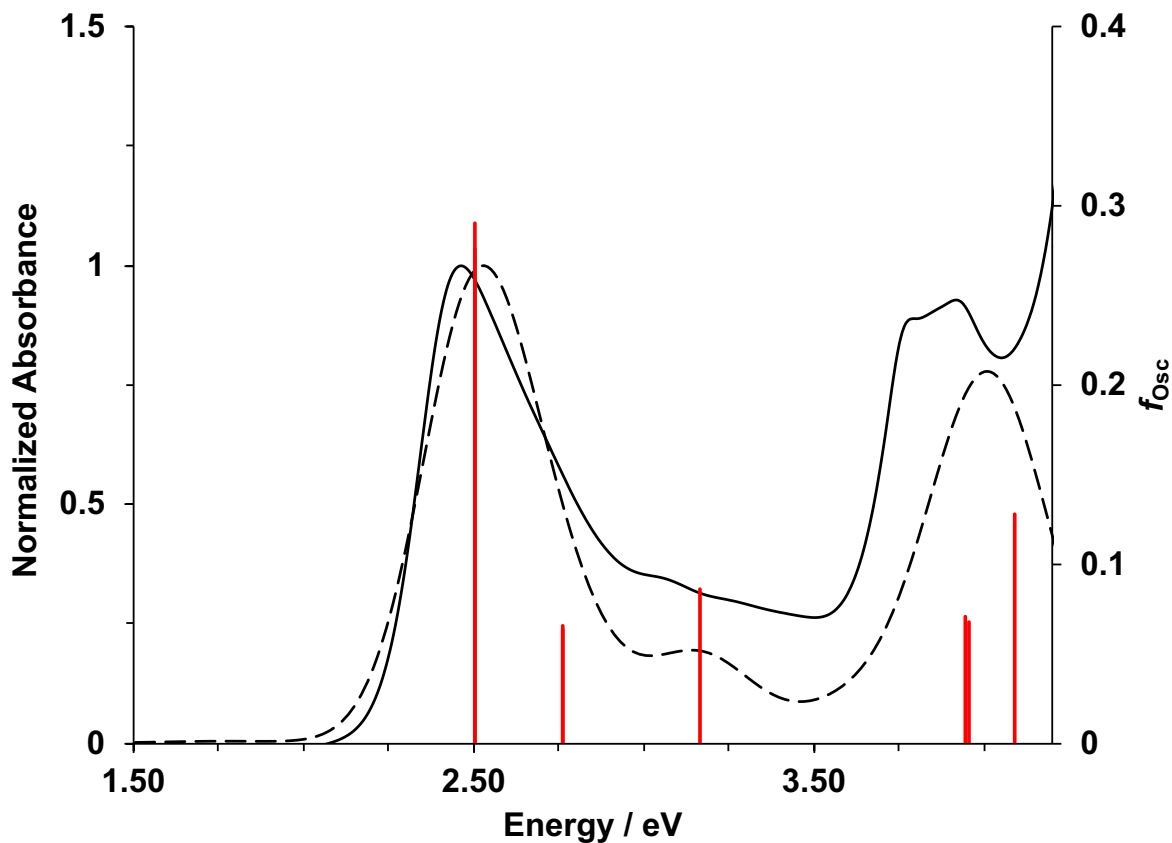


**Figure S12.** TD-DFT simulated spectrum (---) and vertical excitation energies (red) superimposed on the experimental spectrum (-) of  $(^{35}\text{Cl}\text{L})_2\text{Ni}$  in  $\text{CH}_3\text{CN}$  (TD-SMD-uPBE0/6-31+G(d,p)//SMD-uO3LYP/6-31+G(d,p)); FWHM =  $3000 \text{ cm}^{-1}$ ;  $f > 0.05$ .

**Table S7.** TDDFT predicted vertical excitation energies, oscillator strengths ( $f_{\text{osc}} > 0.05$ ), and MO contributions (> 10%) ( ${}^{\text{C}}\text{L}_2\text{Ni}$  (TD-SMD-uPBE0/6-31+G(d,p)//SMD-uO3LYP/6-31+G(d,p)).

No.	E / eV	$f_{\text{osc}}$	Major contribs
<b>10</b>	2.50	0.28	HOMO(A)→LUMO(A) (35%), HOMO(B)→LUMO(B) (33%)
<b>11</b>	2.50	0.29	H-1(A)→LUMO(A) (35%), H-1(B)→LUMO(B) (33%)
<b>18</b>	2.76	0.06	HOMO(A)→L+2(A) (27%), HOMO(A)→L+3(A) (23%), HOMO(B)→L+2(B) (29%), HOMO(B)→L+3(B) (15%)
<b>19</b>	2.76	0.07	H-1(A)→L+2(A) (28%), H-1(A)→L+3(A) (22%), H-1(B)→L+2(B) (25%), H-1(B)→L+3(B) (19%)
<b>29</b>	3.17	0.09	H-1(A)→L+4(A) (12%), H-1(A)→L+5(A) (13%), HOMO(A)→L+4(A) (17%), H-1(B)→L+4(B) (10%), H-1(B)→L+5(B) (10%), HOMO(B)→L+4(B) (15%)
<b>58</b>	3.95	0.07	H-1(B)→L+8(B) (24%)
<b>59</b>	3.96	0.07	H-2(A)→L+4(A) (15%), HOMO(A)→L+8(A) (10%), HOMO(B)→L+9(B) (20%)
<b>70</b>	4.09	0.13	H-5(A)→LUMO(A) (14%), H-2(A)→L+5(A) (19%), H-3(B)→LUMO(B) (13%)

### Equations – IVCT Marcus-Hush Analysis

$$E_{\text{OP}} = \lambda \quad (1)$$

$$H_{ab} (\text{cm}^{-1}) = [(4.2 \times 10^{-4})\epsilon_{\text{max}} \Delta v_{1/2} E_{\text{OP}}]^{1/2} / d \quad (2)$$

$$\Delta G^* (\text{cm}^{-1}) = (\lambda - 2H_{ab})^2 / 4\lambda \quad (3)$$

$$k_{\text{et}} = (2H_{ab}^2 / h)[\pi^3 / \lambda k_B T]^{1/2} \exp(-(\Delta G^* / k_B T)) \quad (4)$$

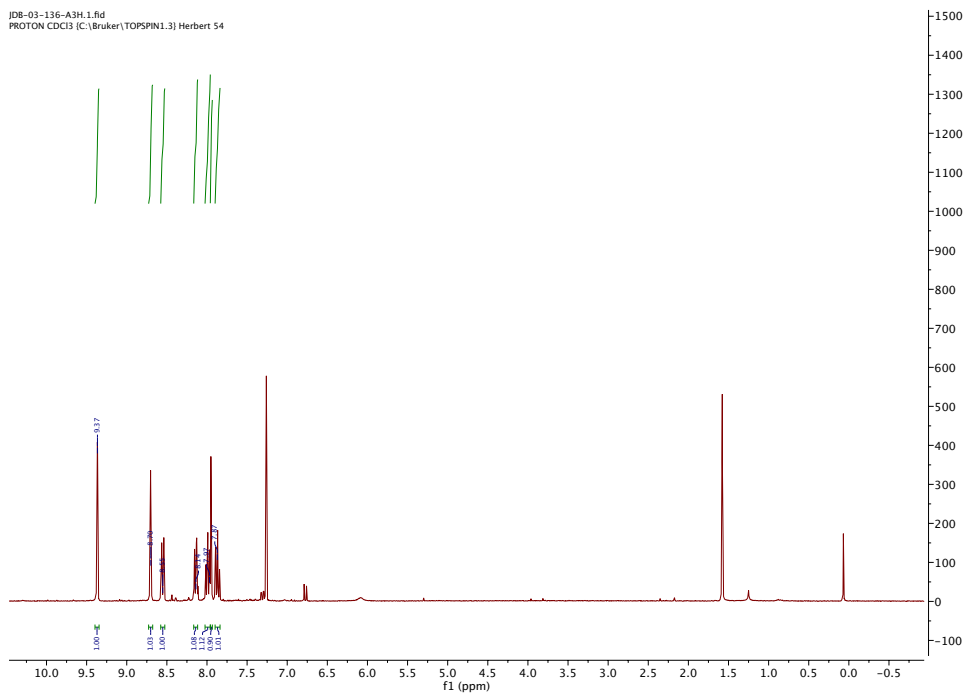


**Figure S13.**  $^1\text{H}$  NMR (300 MHz,  $\text{CDCl}_3$ , 25°C) of 4-nitro-2-chlorophenanthridine (**1c**).

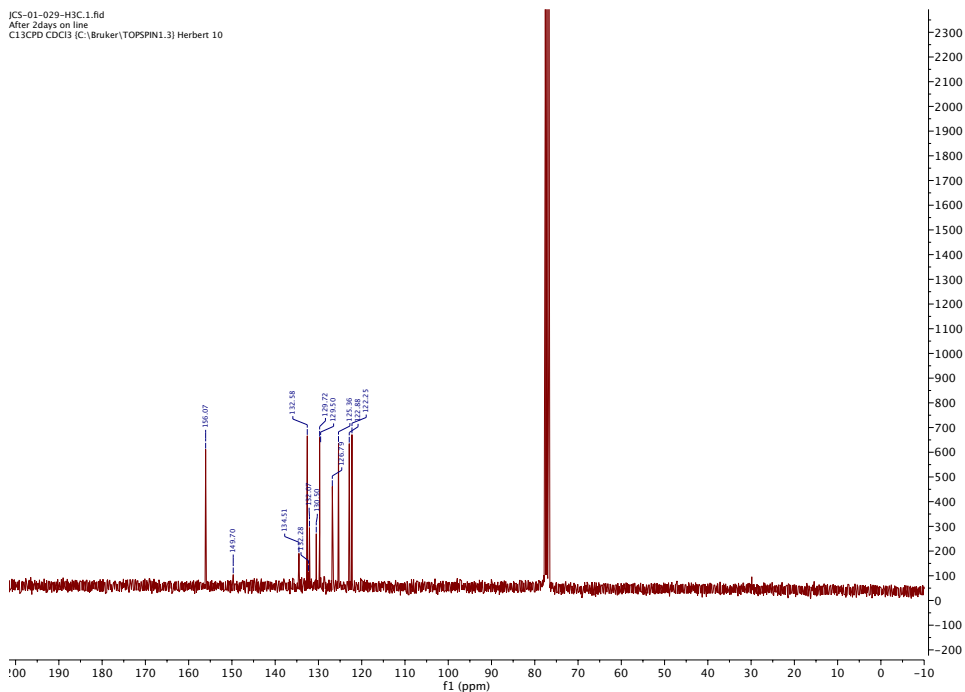


**Figure S14.**  $^{13}\text{C}$  { $^1\text{H}$ } NMR (75 MHz,  $\text{CDCl}_3$ , 25°C) of 4-nitro-2-chlorophenanthridine (**1c**).

JCS-01-031-C3H.1.fid  
Chloroanisole proton  
PROTON CDCl<sub>3</sub> [C:\Bruker\TOPSPIN1.3] Herbert 55

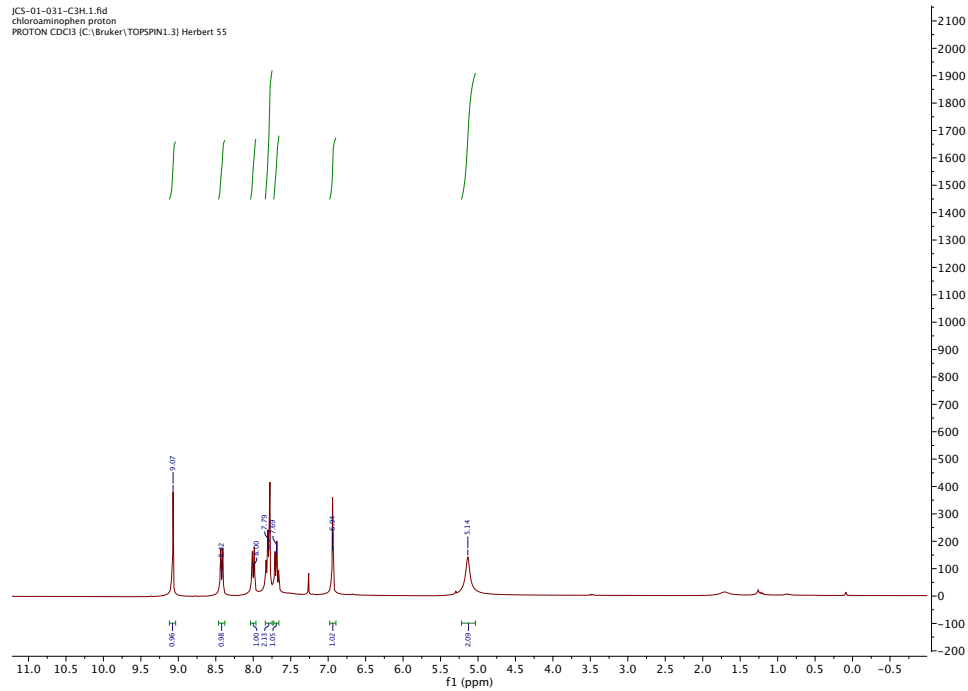


**Figure S15.** <sup>1</sup>H NMR (300 MHz, CDCl<sub>3</sub>, 25°C) of 4-amino-2-chlorophenanthridine (**1e**).

JCS-01-031-C3C.1.fid  
Chloroanisole carbon  
C13CPD CDCl<sub>3</sub> [C:\Bruker\TOPSPIN1.3] Herbert 55

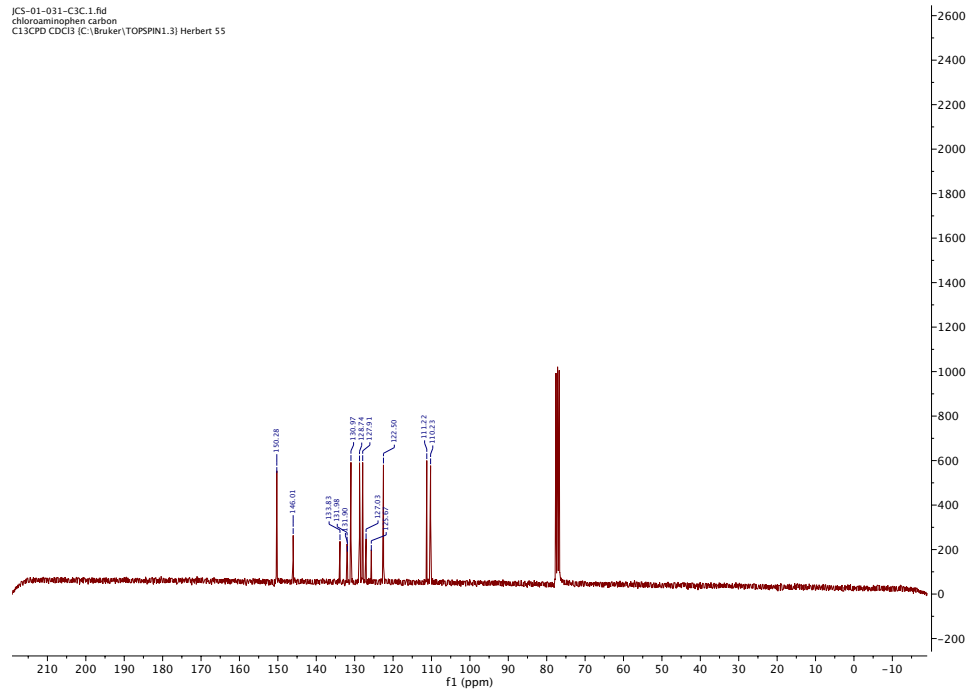


**Figure S16.** <sup>13</sup>C{<sup>1</sup>H} NMR (75 MHz, CDCl<sub>3</sub>, 25°C) of 4-amino-2-chlorophenanthridine (**1e**).

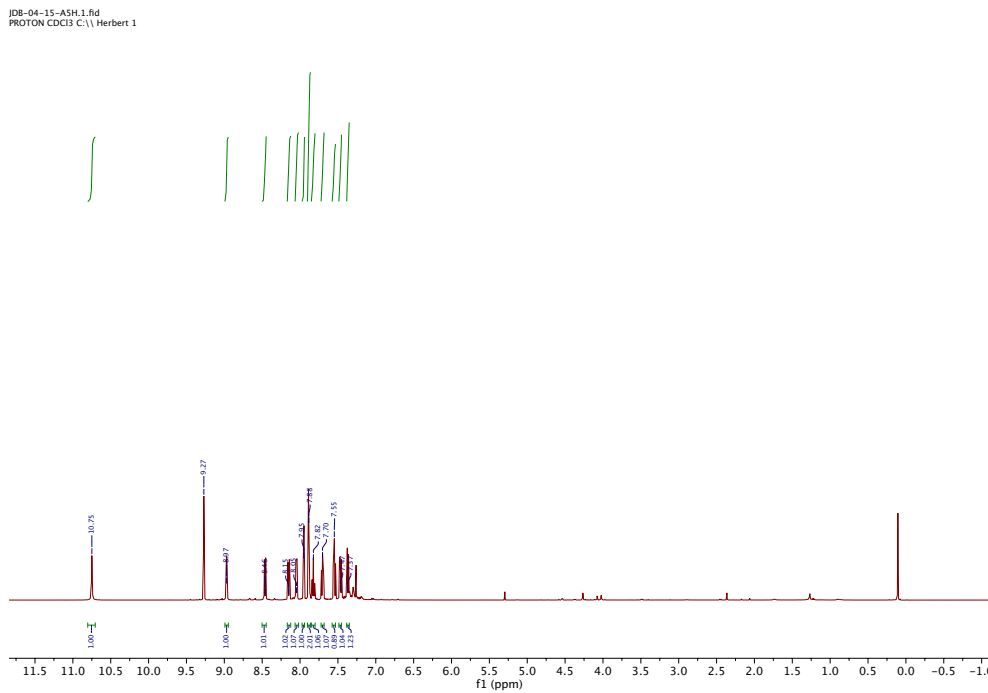


**Figure S17.**  $^1\text{H}$  NMR (500 MHz,  $\text{CDCl}_3$ , 25°C) of  $^{1\text{H}}\text{-PhenNN(H)N}^{\text{Quin}}$  (**L3**).

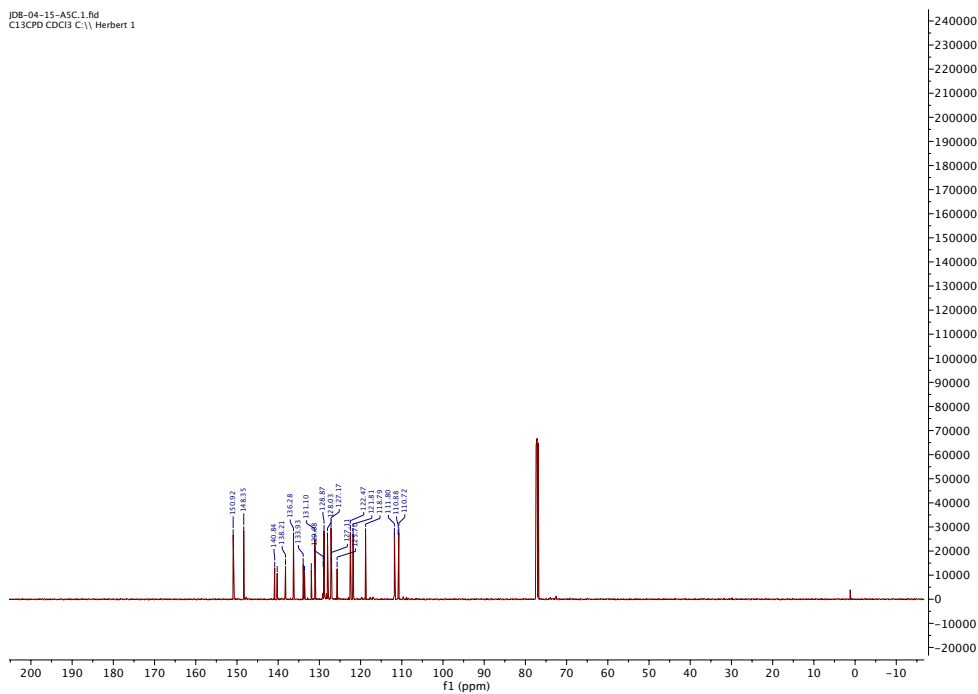


**Figure S18.**  $^{13}\text{C}\{\text{H}\}$  NMR (125 MHz,  $\text{CDCl}_3$ , 25°C) of  $^{\text{Cl-Phen}}\text{NN(H)N}^{\text{Quin}}$  (**L3**).

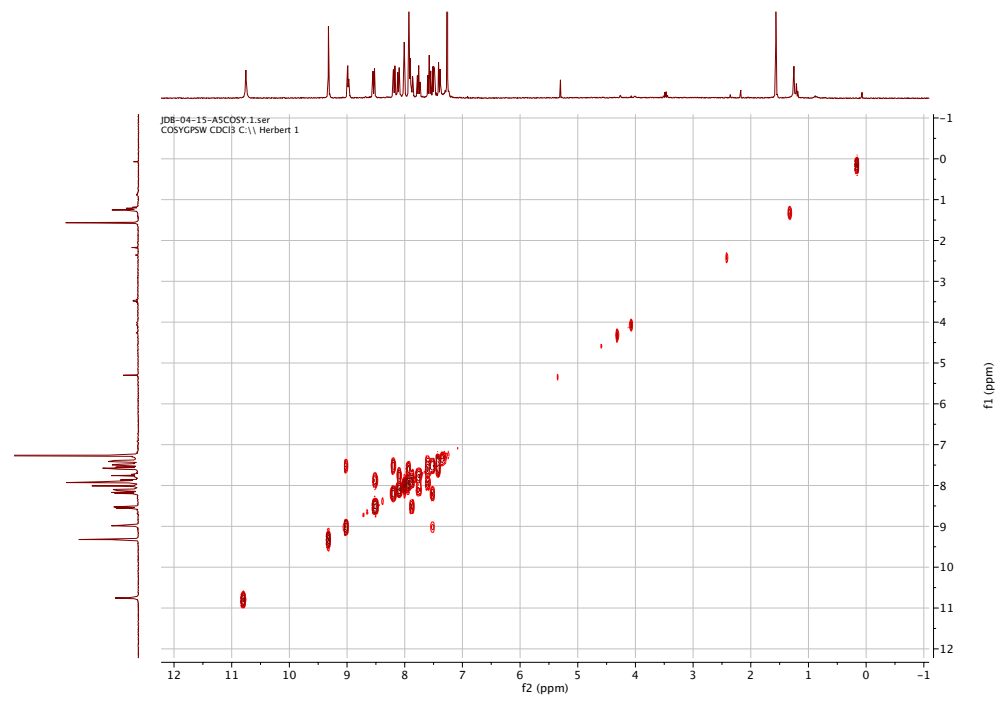


**Figure S19.** <sup>1</sup>H-<sup>1</sup>H COSY NMR (500/125 MHz, CDCl<sub>3</sub>, 25°C) of <sup>Cl</sup>-PhenNN(H)N<sup>Quin</sup> (**L3**).

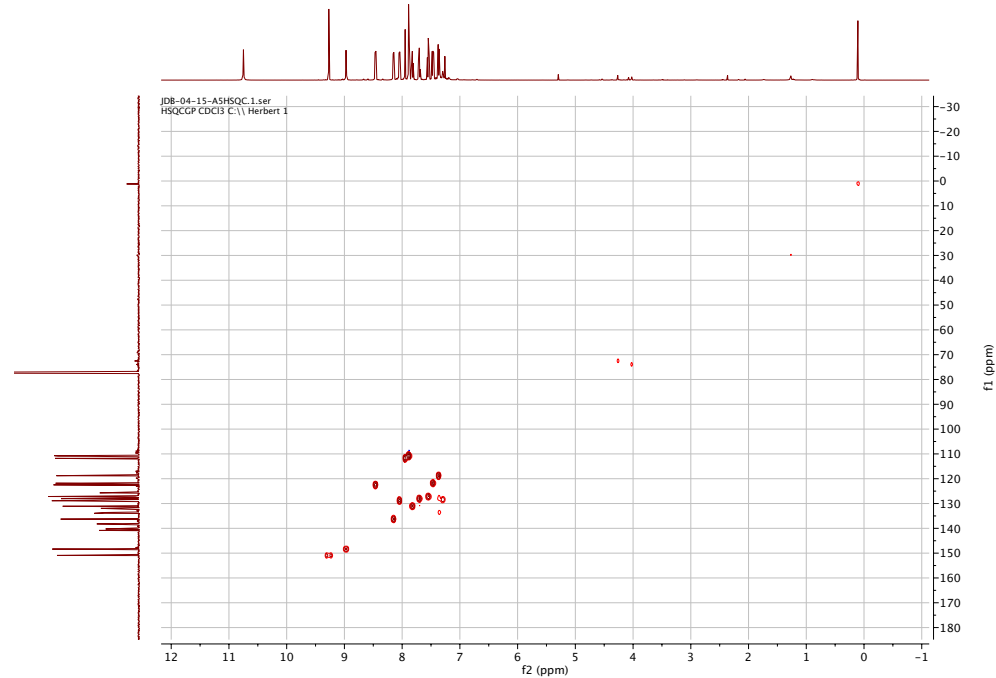


**Figure S20.** HSQC NMR (500/125 MHz, CDCl<sub>3</sub>, 25°C) of <sup>Cl</sup>-PhenNN(H)N<sup>Quin</sup> (**L3**).

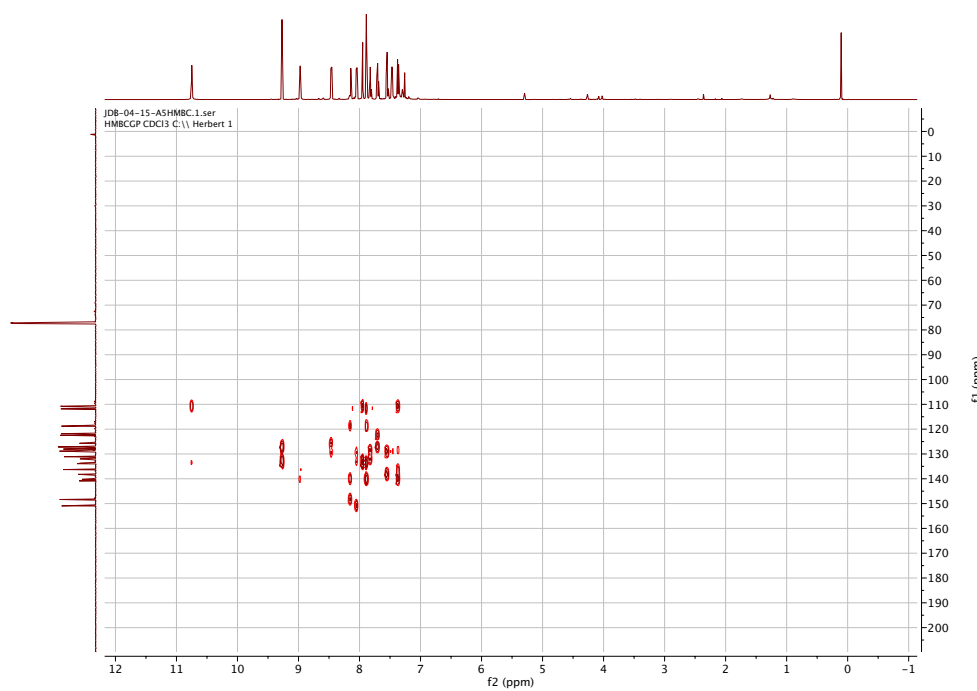
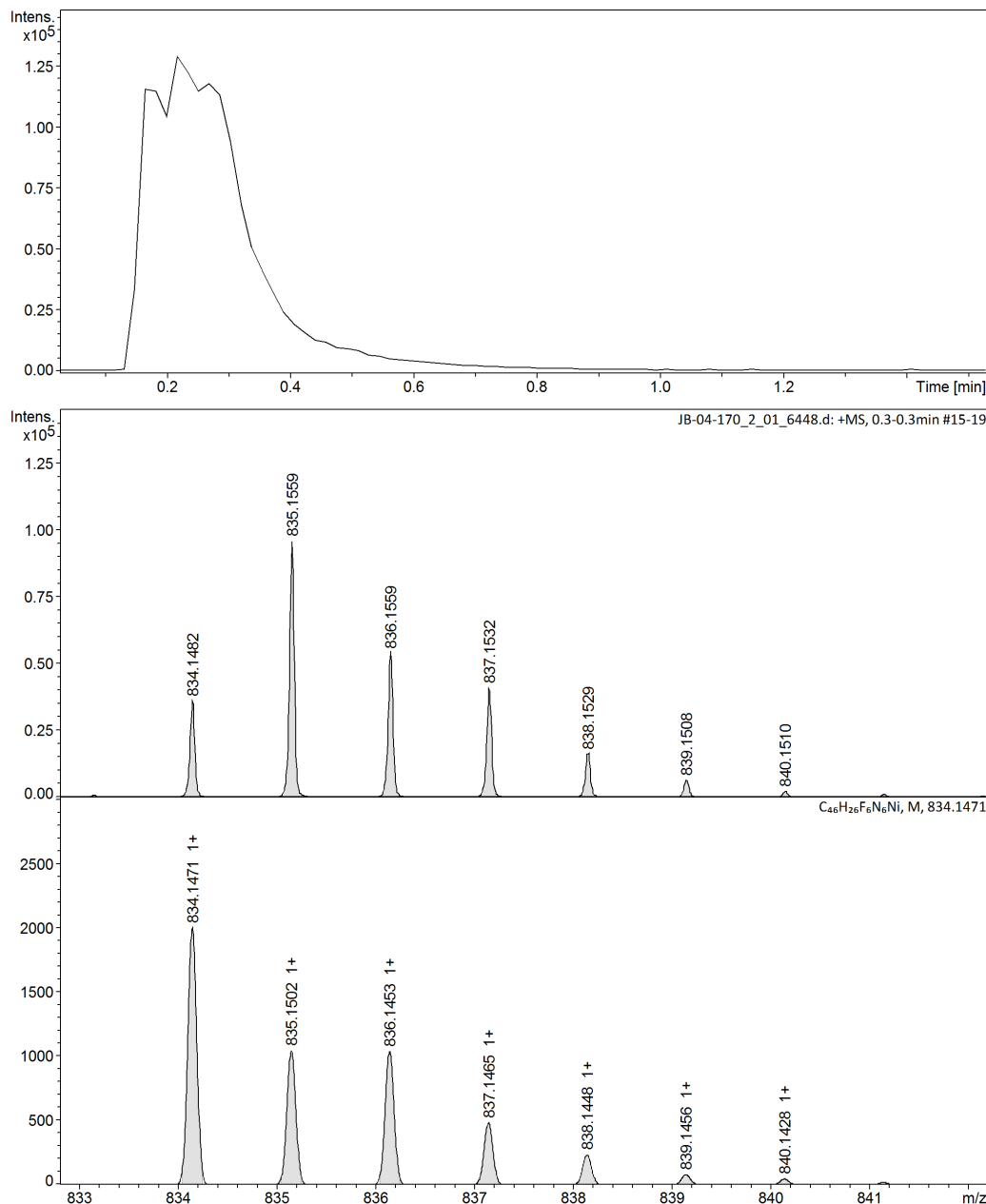


**Figure S21.** HMBC NMR (500/125 MHz, CDCl<sub>3</sub>, 25°C) of <sup>Cl-Phen</sup>NN(H)N<sup>Quin</sup> (**L3**).

### Generic Display Report (all)



Bruker Compass DataAnalysis 4.4

printed: 1/20/2020 2:08:56 PM

by: DA\_users

Page 1 of 1

**Figure S22.** HR-MS of  $(CF_3L)_2Ni$ .

### Generic Display Report (all)

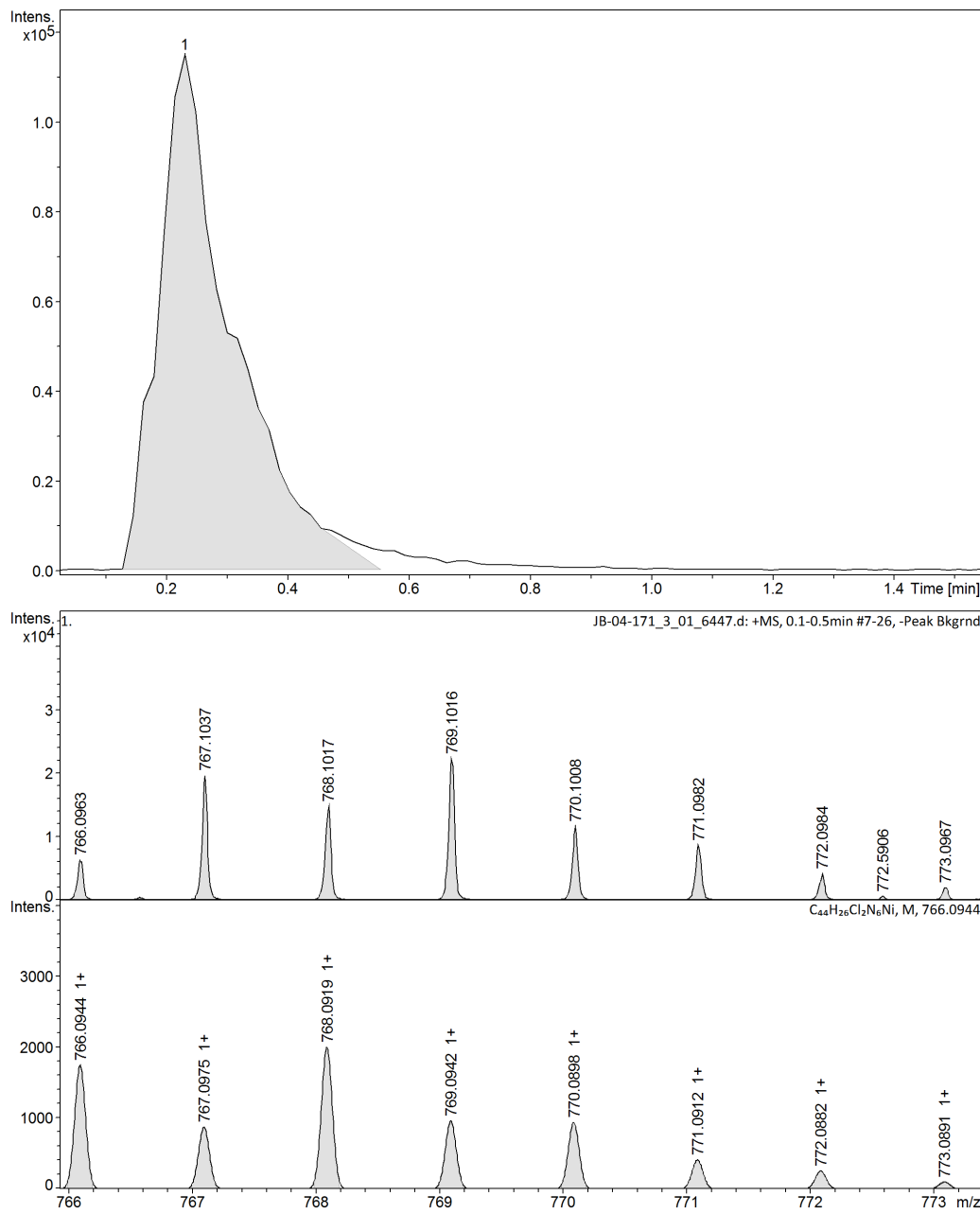
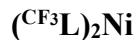


**Figure S23.** HR-MS of  $(\text{ClL})_2\text{Ni}$ .

## Energies and Reaction Coordinates



HF=-4204.0077074 Hartrees  
 Zero-point correction= 0.614886 (Hartree/Particle)  
 Thermal correction to Gibbs Free Energy= 0.532276  
 Sum of electronic and zero-point Energies= -4203.392821  
 Sum of electronic and thermal Free Energies= -4203.475432

Standard orientation:

Center Number	Atomic Number	Atomic Type	Coordinates (Angstroms)		
			X	Y	Z
1	6	0	-0.817190	-2.008570	1.506040
2	1	0	0.213840	-2.344160	1.432690
3	6	0	-1.707190	-2.676860	2.399240
4	6	0	-1.254380	-3.746000	3.209980
5	1	0	-0.211590	-4.046900	3.151430
6	6	0	-2.131630	-4.392830	4.060340
7	1	0	-1.788210	-5.212980	4.684650
8	6	0	-3.480400	-3.981839	4.113570
9	1	0	-4.170330	-4.488759	4.783140
10	6	0	-3.941110	-2.938649	3.324970
11	1	0	-4.983810	-2.651779	3.397920
12	6	0	-3.066440	-2.255889	2.446100
13	6	0	-3.464870	-1.150219	1.589480
14	6	0	-2.466940	-0.534359	0.788160
15	6	0	-2.756820	0.616981	-0.047980
16	6	0	-4.107430	1.011911	-0.122240
17	1	0	-4.411780	1.794231	-0.801550
18	6	0	-5.089390	0.366931	0.646490
19	6	0	-4.794090	-0.674879	1.514490
20	1	0	-5.576790	-1.125269	2.108240
21	6	0	-6.508240	0.856451	0.509020
22	6	0	1.560450	1.538680	-2.974220
23	1	0	2.261140	0.711520	-2.908910
24	6	0	1.814380	2.627110	-3.833530
25	1	0	2.710140	2.630030	-4.446930
26	6	0	0.920470	3.676420	-3.855860
27	1	0	1.094990	4.543800	-4.487700
28	6	0	-0.241110	3.636610	-3.040730
29	6	0	-0.438410	2.470950	-2.235970
30	6	0	-1.620850	2.319680	-1.403660
31	6	0	-2.489630	3.425151	-1.354690
32	1	0	-3.342200	3.425241	-0.689860
33	6	0	-2.265200	4.581150	-2.130400
34	1	0	-2.976620	5.400091	-2.049300
35	6	0	-1.184630	4.695860	-2.984460
36	1	0	-1.034450	5.581910	-3.594470
37	6	0	0.817340	2.008280	1.506280
38	1	0	-0.213690	2.343880	1.433080
39	6	0	1.707440	2.676460	2.399470

40	6	0	1.254730	3.745510	3.210380
41	1	0	0.211940	4.046430	3.151970
42	6	0	2.132060	4.392220	4.060740
43	1	0	1.788710	5.212280	4.685200
44	6	0	3.480830	3.981210	4.113790
45	1	0	4.170830	4.488040	4.783350
46	6	0	3.941450	2.938110	3.325010
47	1	0	4.984150	2.651230	3.397830
48	6	0	3.066690	2.255470	2.446140
49	6	0	3.465020	1.149880	1.589380
50	6	0	2.467010	0.534140	0.788060
51	6	0	2.756780	-0.617110	-0.048240
52	6	0	4.107350	-1.012210	-0.122490
53	1	0	4.411600	-1.794630	-0.801730
54	6	0	5.089400	-0.367340	0.646220
55	6	0	4.794220	0.674480	1.514270
56	1	0	5.576990	1.124830	2.107930
57	6	0	6.508180	-0.857090	0.508820
58	6	0	-1.560330	-1.537430	-2.975040
59	1	0	-2.260910	-0.710200	-2.909540
60	6	0	-1.814280	-2.625530	-3.834760
61	1	0	-2.709920	-2.628089	-4.448340
62	6	0	-0.920560	-3.675010	-3.857240
63	1	0	-1.095150	-4.542170	-4.489350
64	6	0	0.240880	-3.635660	-3.041890
65	6	0	0.438260	-2.470260	-2.236760
66	6	0	1.620640	-2.319400	-1.404290
67	6	0	2.489200	-3.425040	-1.355480
68	1	0	3.341670	-3.425480	-0.690520
69	6	0	2.264680	-4.580800	-2.131540
70	1	0	2.975950	-5.399880	-2.050560
71	6	0	1.184220	-4.695080	-2.985790
72	1	0	1.033970	-5.580930	-3.596070
73	9	0	6.952160	-0.795230	-0.779950
74	9	0	6.643900	-2.163070	0.882860
75	9	0	7.398580	-0.157000	1.250580
76	7	0	-1.172570	-1.001900	0.747690
77	7	0	-1.691930	1.136820	-0.719010
78	7	0	0.482410	1.466060	-2.205870
79	7	0	1.172640	1.001700	0.747770
80	7	0	1.691880	-1.136700	-0.719420
81	7	0	-0.482410	-1.465250	-2.206470
82	28	0	-0.000040	0.000070	-0.731030
83	9	0	-6.952370	0.793931	-0.779650
84	9	0	-6.644090	2.162601	0.882480
85	9	0	-7.398490	0.156661	1.251280

### (<sup>C</sup>L)<sub>2</sub>Ni

HF= -4449.2607093 Hartrees  
 Zero-point correction= 0.588006 (Hartree/Particle)  
 Thermal correction to Gibbs Free Energy= 0.513597  
 Sum of electronic and zero-point Energies= -4448.672704  
 Sum of electronic and thermal Free Energies= -4448.747113

Standard orientation:

Center Number	Atomic Number	Atomic Type	Coordinates (Angstroms)		
			X	Y	Z
1	6	0	0.412885	2.445825	0.548616
2	1	0	-0.600347	2.434041	0.940363
3	6	0	1.101572	3.690218	0.429336
4	6	0	0.469470	4.907731	0.781412
5	1	0	-0.556440	4.884322	1.139741
6	6	0	1.151701	6.104660	0.667188
7	1	0	0.668422	7.040314	0.934476
8	6	0	2.483052	6.105690	0.199677
9	1	0	3.019712	7.046319	0.107566
10	6	0	3.118331	4.922896	-0.145941
11	1	0	4.140864	4.965296	-0.503126
12	6	0	2.444802	3.682062	-0.041640
13	6	0	3.038145	2.399026	-0.384276
14	6	0	2.225627	1.237930	-0.271389
15	6	0	2.718490	-0.079184	-0.635927
16	6	0	4.081113	-0.163231	-0.999265
17	1	0	4.554011	-1.114881	-1.183722
18	6	0	4.858769	0.995040	-1.072628
19	6	0	4.380730	2.266809	-0.808259
20	1	0	5.030710	3.125354	-0.907261
21	6	0	-1.036466	-3.544947	0.785724
22	1	0	-1.805989	-3.064459	1.382159
23	6	0	-1.082284	-4.932039	0.539469
24	1	0	-1.884495	-5.527309	0.964599
25	6	0	-0.108435	-5.495547	-0.256946
26	1	0	-0.121745	-6.558222	-0.486204
27	6	0	0.921477	-4.683810	-0.800337
28	6	0	0.911834	-3.294158	-0.460947
29	6	0	1.942299	-2.390150	-0.947763
30	6	0	2.871750	-2.942403	-1.848429
31	1	0	3.609105	-2.317612	-2.331440
32	6	0	2.855126	-4.310246	-2.190973
33	1	0	3.606378	-4.673680	-2.888690
34	6	0	1.925193	-5.188261	-1.668228
35	1	0	1.933444	-6.243872	-1.923813
36	6	0	-0.961725	-0.501634	-2.470447
37	1	0	0.022204	-0.885203	-2.725440
38	6	0	-1.882672	-0.188634	-3.514976
39	6	0	-1.542317	-0.401744	-4.873073
40	1	0	-0.566707	-0.816974	-5.112598
41	6	0	-2.441945	-0.085111	-5.873937
42	1	0	-2.184080	-0.248615	-6.916620
43	6	0	-3.701294	0.453386	-5.534236
44	1	0	-4.409671	0.700689	-6.320542
45	6	0	-4.049640	0.671463	-4.210224
46	1	0	-5.026898	1.084657	-3.987943
47	6	0	-3.150056	0.355877	-3.163786
48	6	0	-3.438068	0.555249	-1.752310
49	6	0	-2.454281	0.152769	-0.808620
50	6	0	-2.672484	0.273792	0.622304
51	6	0	-3.864357	0.916043	1.025413
52	1	0	-4.055312	1.139501	2.063107

53	6	0	-4.797867	1.324002	0.069500
54	6	0	-4.640807	1.140439	-1.293486
55	1	0	-5.412889	1.458254	-1.980731
56	6	0	1.912981	-0.988868	2.970274
57	1	0	2.713928	-1.079208	2.242801
58	6	0	2.176933	-1.133631	4.347355
59	1	0	3.192485	-1.319104	4.683364
60	6	0	1.125499	-1.052822	5.235106
61	1	0	1.286316	-1.179861	6.302859
62	6	0	-0.189859	-0.815208	4.757254
63	6	0	-0.355611	-0.637735	3.347512
64	6	0	-1.661724	-0.362487	2.769460
65	6	0	-2.750092	-0.391278	3.661034
66	1	0	-3.763130	-0.295329	3.297332
67	6	0	-2.573041	-0.589325	5.045938
68	1	0	-3.456384	-0.594193	5.680742
69	6	0	-1.324645	-0.772008	5.609092
70	1	0	-1.198054	-0.905191	6.679605
71	17	0	6.551801	0.817236	-1.534169
72	17	0	-6.264436	2.118230	0.643724
73	7	0	0.938656	1.294143	0.213318
74	7	0	1.821193	-1.096273	-0.515844
75	7	0	-0.078804	-2.761421	0.309152
76	7	0	-1.232667	-0.347089	-1.198409
77	7	0	-1.662108	-0.183831	1.411890
78	7	0	0.700104	-0.747592	2.491885
79	28	0	0.081646	-0.642936	0.453618

### (tBuL)<sub>2</sub>Ni (S = 3/2)

HF= -3844.3447266 Hartrees

Zero-point correction= 0.832030 (Hartree/Particle)

Thermal correction to Gibbs Free Energy= 0.748612

Sum of electronic and zero-point Energies= -3843.512697

Sum of electronic and thermal Free Energies= -3843.596114  
Standard orientation:

Center Number	Atomic Number	Atomic Type	Coordinates (Angstroms)		
			X	Y	Z
1	6	0	-0.072980	-2.125885	-1.118922
2	1	0	0.968553	-1.949422	-1.370435
3	6	0	-0.636700	-3.415059	-1.356675
4	6	0	0.158275	-4.468329	-1.871209
5	1	0	1.209473	-4.283382	-2.076868
6	6	0	-0.400416	-5.711235	-2.103254
7	1	0	0.206402	-6.522394	-2.495744
8	6	0	-1.767682	-5.922518	-1.825362
9	1	0	-2.206943	-6.900517	-2.004059
10	6	0	-2.561639	-4.901583	-1.325753
11	1	0	-3.606686	-5.105694	-1.122790
12	6	0	-2.018485	-3.617952	-1.077255
13	6	0	-2.777526	-2.492901	-0.555420
14	6	0	-2.079473	-1.285430	-0.299101

15	6	0	-2.758958	-0.145566	0.271645
16	6	0	-4.152309	-0.249330	0.436170
17	1	0	-4.706973	0.619160	0.754282
18	6	0	-4.869607	-1.429781	0.149974
19	6	0	-4.168777	-2.544573	-0.309266
20	1	0	-4.696149	-3.465357	-0.509526
21	6	0	-6.400410	-1.444812	0.355052
22	6	0	-6.727019	-1.146597	1.837502
23	1	0	-7.811094	-1.169231	1.994257
24	1	0	-6.368090	-0.161587	2.148307
25	1	0	-6.275887	-1.895181	2.497988
26	6	0	-7.032626	-2.801563	-0.006737
27	1	0	-6.869895	-3.065111	-1.056805
28	1	0	-8.113979	-2.750581	0.155288
29	1	0	-6.646441	-3.615482	0.615318
30	6	0	-7.050342	-0.362900	-0.540042
31	1	0	-6.838594	-0.549126	-1.598630
32	1	0	-6.696627	0.642851	-0.296414
33	1	0	-8.137838	-0.372138	-0.407679
34	6	0	0.771121	3.826815	0.234602
35	1	0	1.656600	3.564200	-0.334983
36	6	0	0.641542	5.111305	0.798311
37	1	0	1.424943	5.846396	0.643284
38	6	0	-0.475548	5.394290	1.555069
39	1	0	-0.600732	6.366566	2.024753
40	6	0	-1.472778	4.402427	1.740447
41	6	0	-1.279729	3.144671	1.090783
42	6	0	-2.263909	2.080384	1.203334
43	6	0	-3.344269	2.320761	2.075262
44	1	0	-4.055075	1.538490	2.296865
45	6	0	-3.510458	3.558359	2.724547
46	1	0	-4.368311	3.684627	3.380608
47	6	0	-2.620767	4.602932	2.550764
48	1	0	-2.770362	5.560968	3.039941
49	6	0	0.658210	0.085775	2.652307
50	1	0	-0.367698	0.354685	2.888543
51	6	0	1.495790	-0.438893	3.681403
52	6	0	1.012275	-0.574571	5.005497
53	1	0	-0.006512	-0.268558	5.228407
54	6	0	1.831070	-1.087360	5.993983
55	1	0	1.465486	-1.191437	7.011634
56	6	0	3.149291	-1.476170	5.674362
57	1	0	3.793871	-1.877082	6.452178
58	6	0	3.638175	-1.354501	4.382641
59	1	0	4.657570	-1.661774	4.179486
60	6	0	2.824411	-0.832356	3.349170
61	6	0	3.250629	-0.669123	1.969316
62	6	0	2.336737	-0.083906	1.060895
63	6	0	2.722124	0.154386	-0.309299
64	6	0	3.967075	-0.339687	-0.735893
65	1	0	4.220434	-0.275433	-1.783673
66	6	0	4.872747	-0.965113	0.144704
67	6	0	4.513956	-1.089413	1.487614
68	1	0	5.201905	-1.549701	2.181444
69	6	0	6.214661	-1.494469	-0.404886
70	6	0	5.936666	-2.564750	-1.487153
71	1	0	5.371409	-3.406266	-1.072137

72	1	0	6.883048	-2.954434	-1.877580
73	1	0	5.371865	-2.161163	-2.332360
74	6	0	7.087735	-2.138047	0.688012
75	1	0	7.351234	-1.426459	1.477234
76	1	0	8.021801	-2.491780	0.240469
77	1	0	6.599218	-3.001051	1.151744
78	6	0	7.014273	-0.327303	-1.030264
79	1	0	6.483875	0.134377	-1.867647
80	1	0	7.974898	-0.693378	-1.408504
81	1	0	7.219322	0.451589	-0.287818
82	6	0	-1.636263	1.707085	-2.895668
83	1	0	-2.533554	1.511309	-2.316681
84	6	0	-1.728020	2.219635	-4.204823
85	1	0	-2.704735	2.402642	-4.641244
86	6	0	-0.565953	2.494862	-4.894696
87	1	0	-0.595844	2.909974	-5.898620
88	6	0	0.688868	2.246194	-4.282594
89	6	0	0.681599	1.685387	-2.972037
90	6	0	1.925500	1.366717	-2.293763
91	6	0	3.118948	1.761440	-2.927578
92	1	0	4.067519	1.658189	-2.418630
93	6	0	3.109596	2.341180	-4.208576
94	1	0	4.057893	2.624886	-4.657230
95	6	0	1.930321	2.558371	-4.899691
96	1	0	1.935348	2.993616	-5.894726
97	7	0	-0.748076	-1.124772	-0.609004
98	7	0	-1.961780	0.946289	0.505395
99	7	0	-0.154580	2.885060	0.369575
100	7	0	1.054037	0.262947	1.415866
101	7	0	1.769984	0.779985	-1.071563
102	7	0	-0.477876	1.445902	-2.303129
103	28	0	-0.093226	0.862983	-0.280212